

## Supporting Information

Warming leads to changes in soil organic carbon molecules due to decreased mineral protection

Li Zhang<sup>1,2#</sup>, Ruilin Huang<sup>3#</sup>, Zhiyuan Ma<sup>1#</sup>, Sen Li<sup>1</sup>, Jixian Ding<sup>1</sup>, Weigen Huang<sup>1,2</sup>, Chaoyang Liu<sup>1,2</sup>, Yueyu Sui<sup>4</sup>, Jizhong Zhou<sup>5</sup>, Jiabao Zhang<sup>1</sup>, Yuting Liang<sup>1,2\*</sup>

<sup>1</sup> State Key Laboratory of Soil and Sustainable Agriculture, Institute of Soil Science, Chinese Academy of Sciences, Nanjing 210008, China.

<sup>2</sup> University of Chinese Academy of Sciences, Beijing 100049, China.

<sup>3</sup> College of Resource and Environment, Anhui Science and Technology University, Chuzhou 233100, China.

<sup>4</sup> Northeast Institute of Geography and Agricultural Ecology, Chinese Academy of Sciences, Harbin 150040, China.

<sup>5</sup> School of Biological Sciences, University of Oklahoma, Oklahoma, 73069, USA

#The first three authors contributed equally.

\*To whom correspondence may be addressed: Yuting Liang, ytliang@issas.ac.cn

The authors declare no conflicts of interest.

Appendix: Table S1-S2

**Table S1.** Assignment of  $^{13}\text{C}$  NMR signal intensity in the chemical shift regions associated with each component of the molecular mixing model and the empirical molar ratio of N/C in soils.

Chemical shift region (ppm)	Carbohydrate	Protein	Lignin	Lipid	Carbonyl	Char
0-45	0.0	35.4	10.5	75.6	0.0	1.3
45-60	0.0	22.6	13.8	4.5	0.0	1.2
60-95	83.3	3.5	12.5	9.0	0.0	1.3
95-110	16.7	0.0	8.6	0.0	0.0	6.3
110-145	0.0	8.9	30.6	3.6	0.0	64.9
145-165	0.0	1.3	19.5	0.7	0.0	17.5
165-210	0.0	28.3	4.6	6.6	100.0	7.7
Molar N:C	0.0	0.27	0.0	0.0	0.0	0.0

**Table S2.** Permutational multivariate analysis of variance (PERMANOVA) of translocated warming and SOC gradient for different organic carbon molecules.

	df	R <sup>2</sup>	F value	<i>p</i>
Warming	5	0.21	124	< 0.001
SOC gradient	4	0.53	393	< 0.001
Warming × SOC gradient	20	0.24	36	< 0.001

Appendix: Figure S1-S16

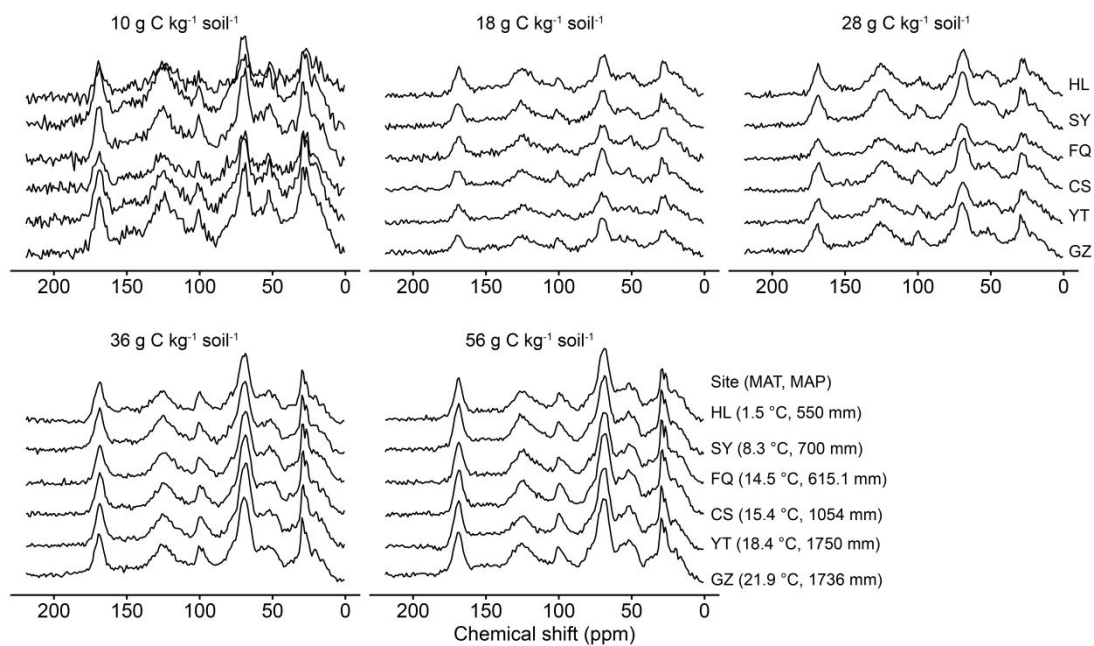


**Fig. S1.** NMR spectra of different sites under different organic carbon contents and climatic conditions of different sites.

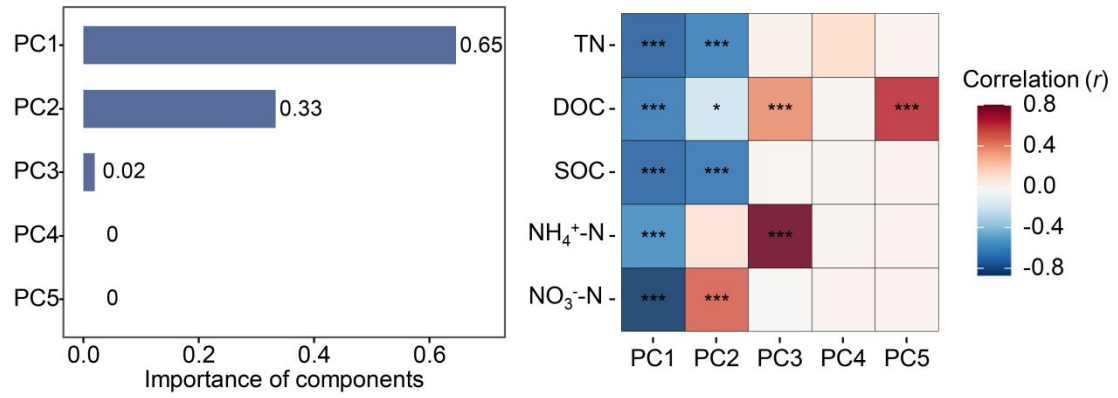


**Fig. S2.** The amount of explanation of the nutrient matrix by the PC axis in the principal component analysis and the correlation between the PC axis and the nutrient factors.

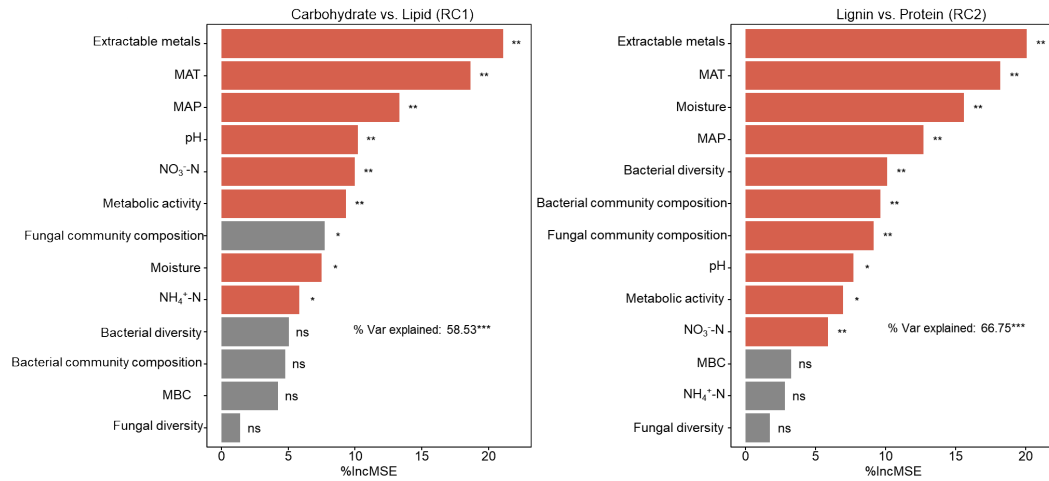


**Fig. S3.** Random forest analysis of the importance of different factors for RC1 and RC2. The response variables for carbohydrate vs. lipid and lignin vs. protein are represented by the RC1 and RC2 axes in Fig. 2. Significance is indicated by <sup>ns</sup> $p > 0.05$ , \* $p < 0.05$ , \*\* $p < 0.01$ , and \*\*\* $p < 0.001$ .

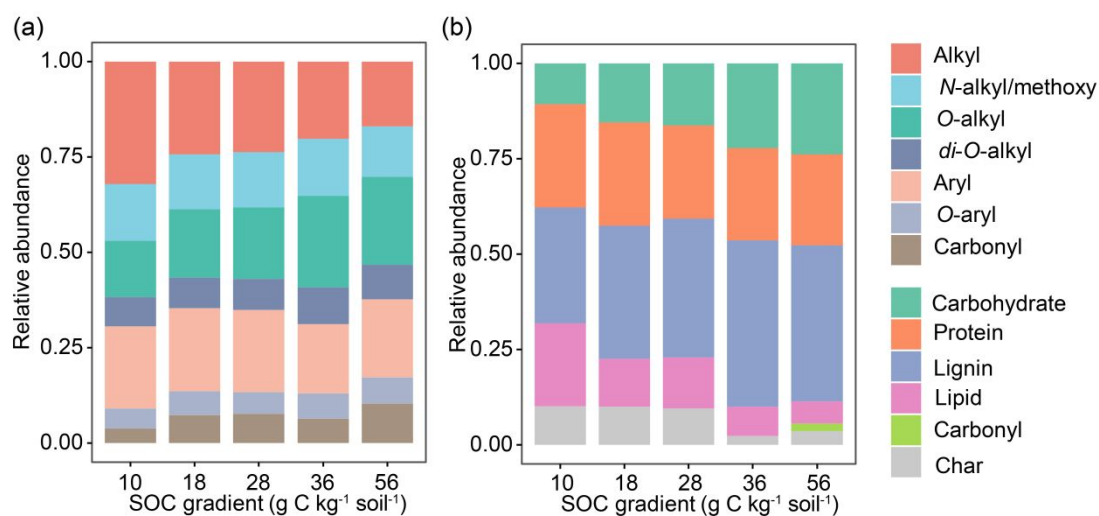


**Fig. S4.** Relative abundance of functional groups (a) and constituent molecules (b) in the organic C composition for soils with different initial SOC contents at the *in situ* sites (HL,  $n_{\text{sample}} = 15$ ). It should be noted that this analysis only involves the analysis of the *in situ* sites; the other analyses include both the *in situ* sites and the five translocated sites.

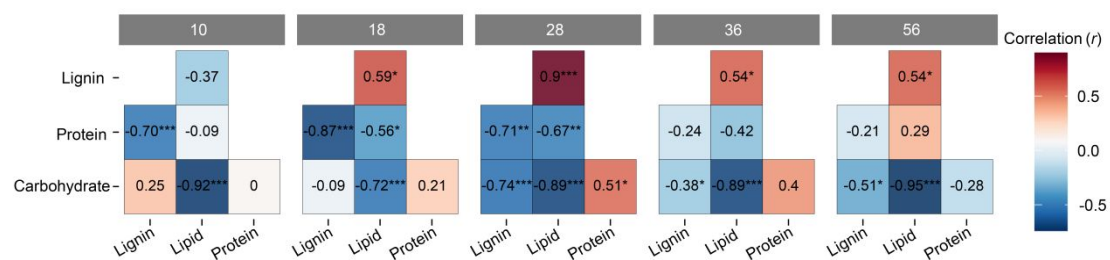


**Fig. S5.** Correlation between the four main constituent molecules in soils with different initial SOC contents (10~56 g C kg<sup>-1</sup> soil<sup>-1</sup>). Colors represent Pearson correlations ( $n_{\text{sample}} = 90$ ). Blue represents a negative correlation, and red represents a positive correlation. Significance is presented by \* $p < 0.05$ , \*\* $p < 0.01$ , and \*\*\* $p < 0.001$ .



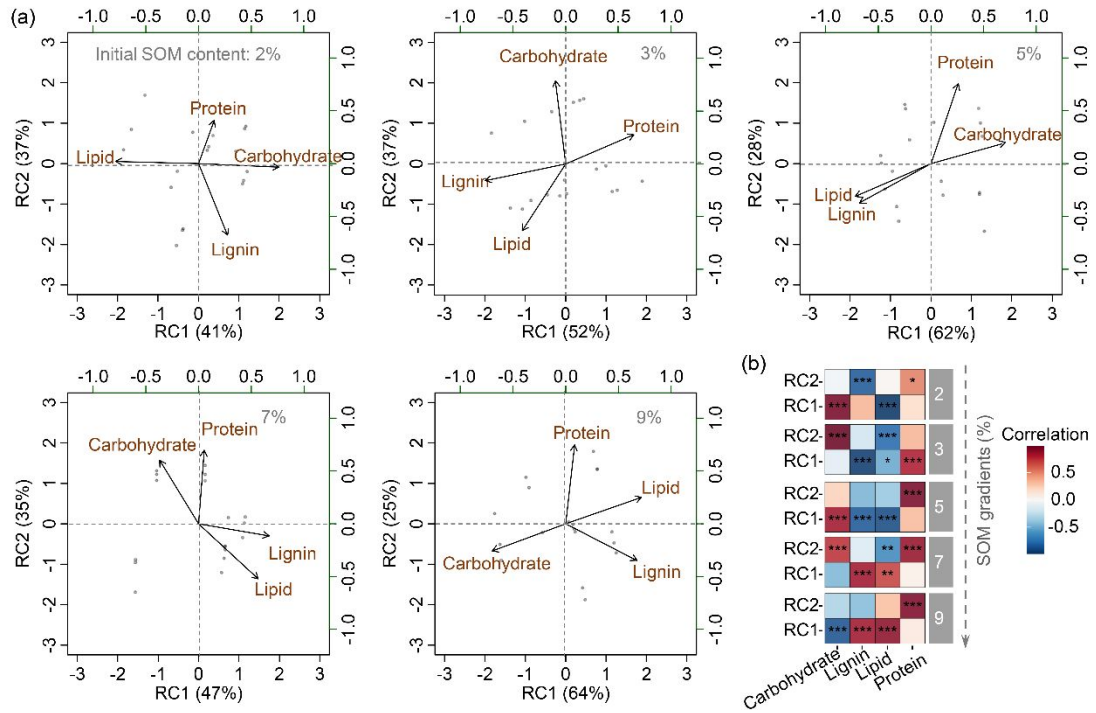


**Fig. S6.** Rotational principal component analysis of SOC molecules (a) and correlation analysis of the leading RC axes with the relative abundance of C molecules (b). RC1 and RC2 represent rotated components 1-2; panels indicate pairwise comparisons of RC1 and RC2. Grey dots represent soil samples, and labelled arrows indicate correlations between SOC molecules and RCs. Colors represent Pearson correlations in correlation analysis. Blue represents negative correlation and red represents positive correlation. Significance is presented by \* $p < 0.05$ , \*\* $p < 0.01$ , and \*\*\* $p < 0.001$ .

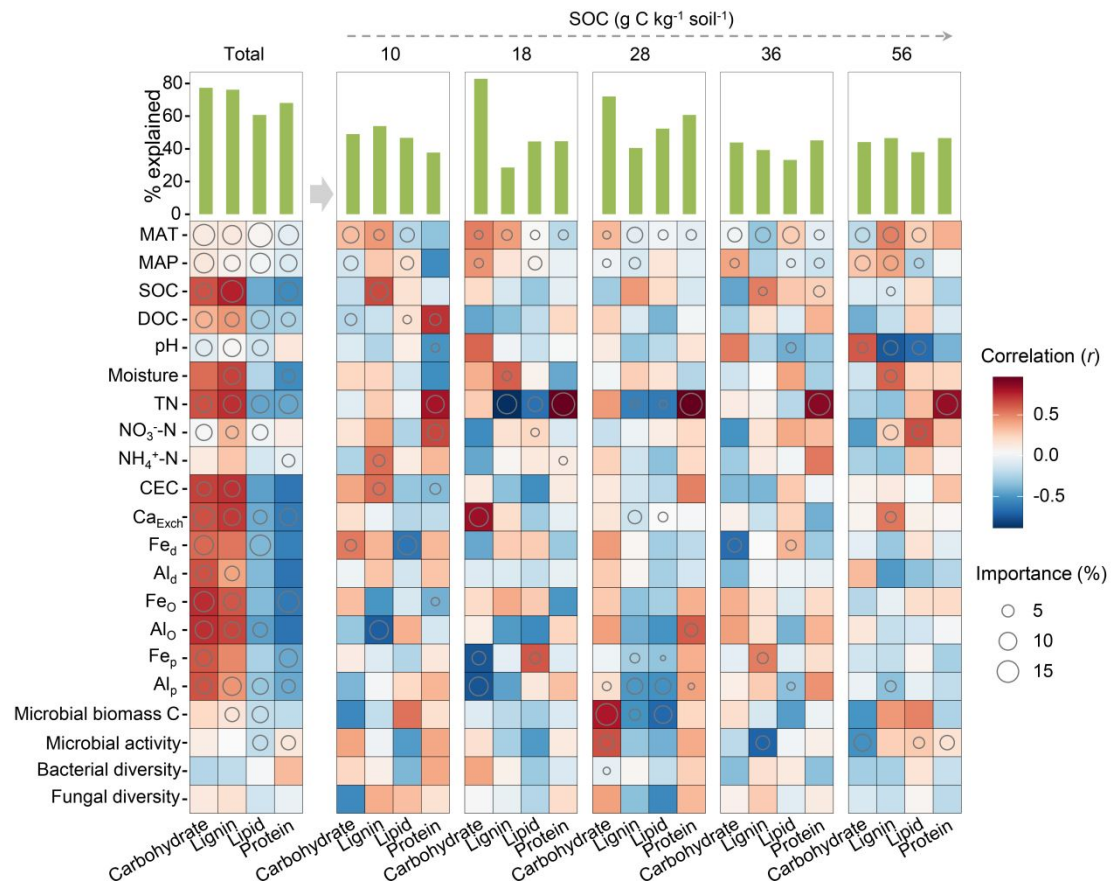


**Fig. S7.** Contribution of biogeochemical variables to four molecular abundance changes based on correlation analysis and random forest models. Colors represent Pearson correlations ( $n_{\text{sample}} = 90$ ). Blue represents a negative correlation, and red represents a positive correlation. The circle size represents the importance of the variables in the random forest model, in which only the significantly ( $p < 0.05$ ) important circles are displayed. In the bar plot, the height of the bars represents the explained amount of biogeochemical variables on changes in the abundance of constituent molecules.

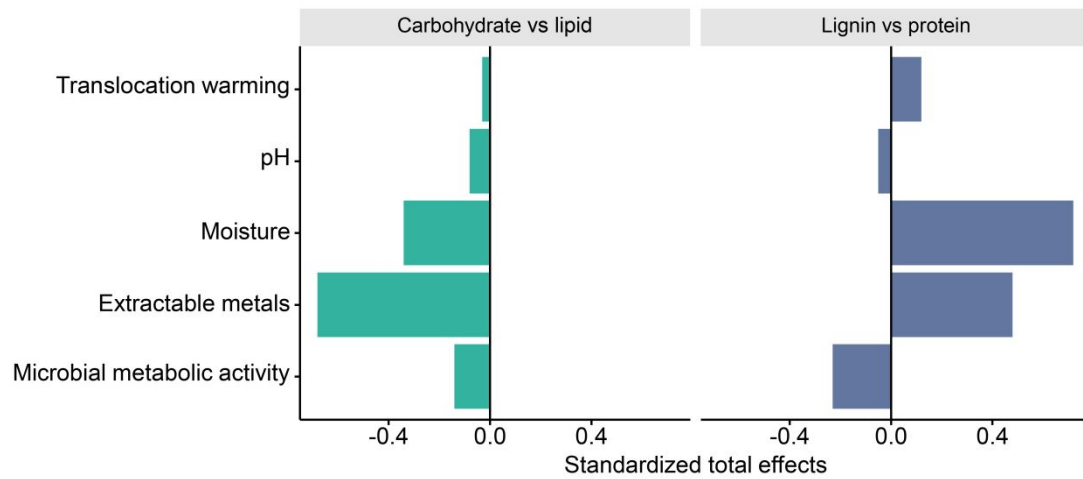


**Fig. S8.** Standard total effects of different biogeochemical variables on carbohydrate-lipid trade-off and lignin-protein trade-off in SEMs (Fig. 3). Here, “Translocation warming” represents “Climatic regimes” in Fig. 3.

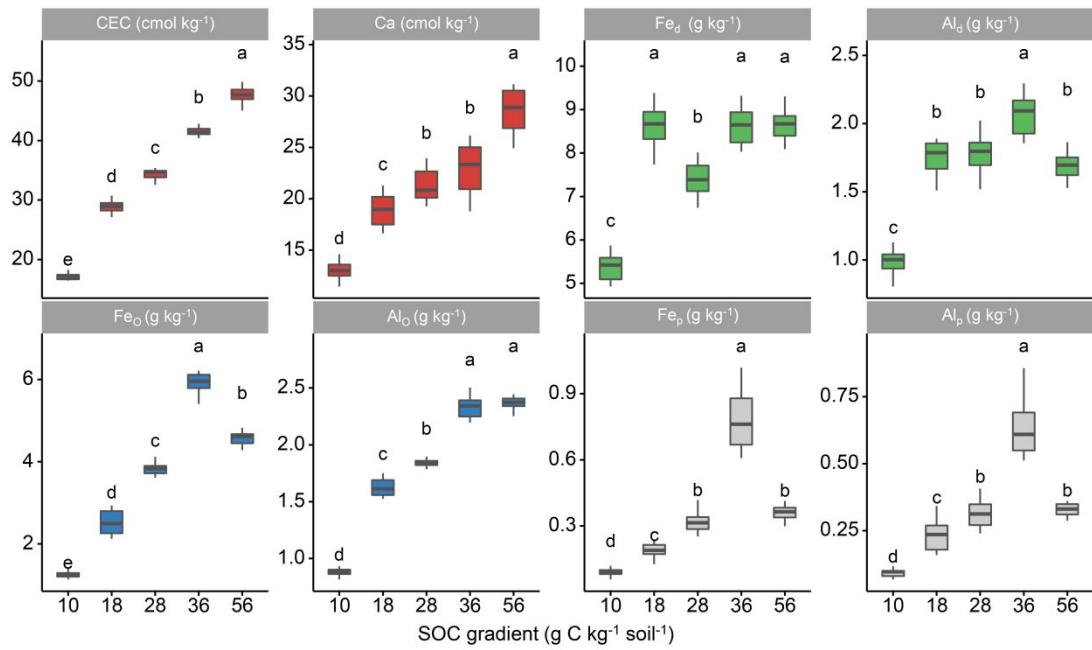


**Fig. S9.** Content of different extractable metals in the unit soil. The content differences for different extractable metals among soils with different organic carbon contents were statistically determined using the Tukey HSD method. Different lowercase letters indicate significant differences, and the same lowercase letters indicate nonsignificant differences.

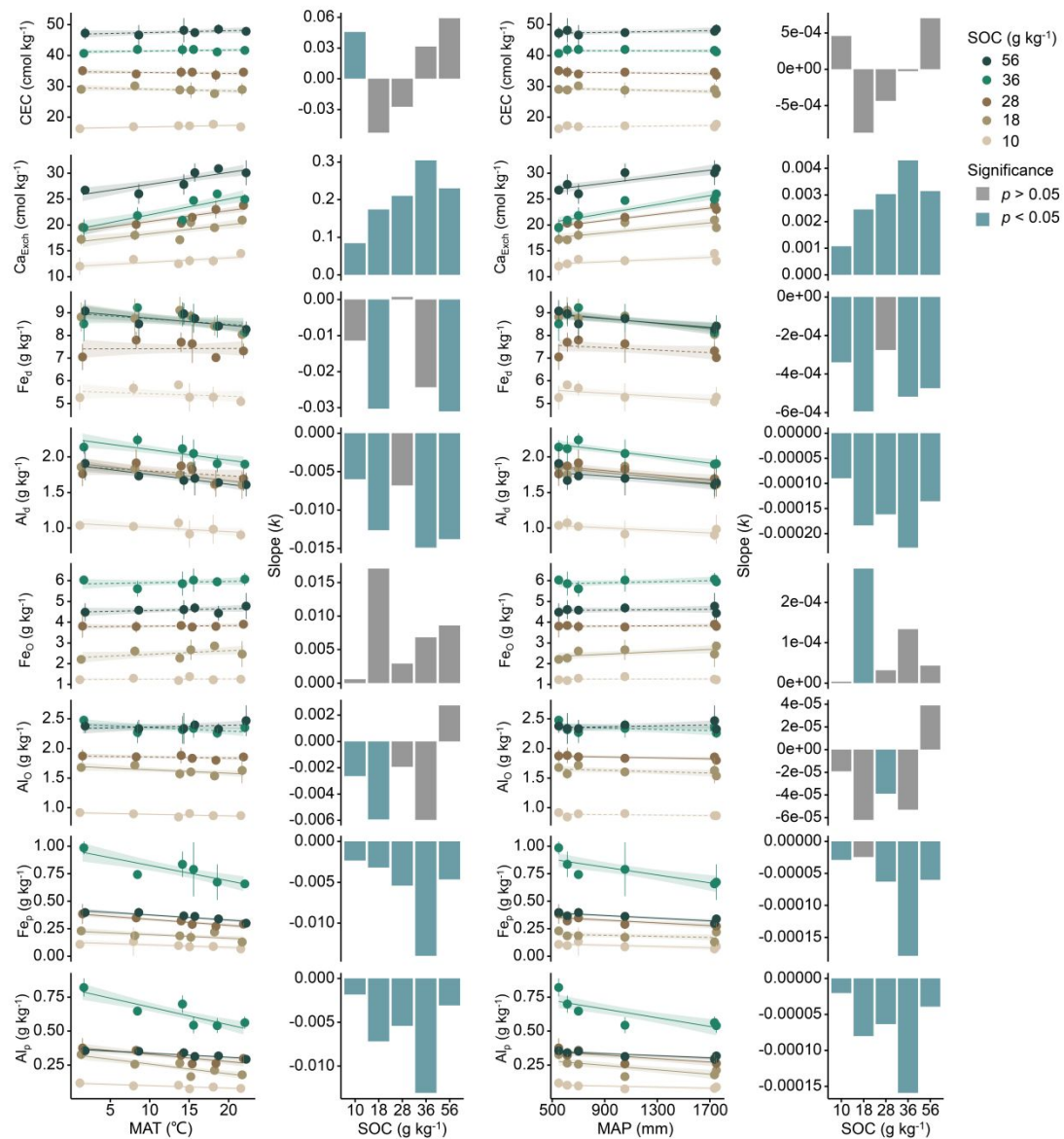


**Fig. S10.** Linear fitting analysis between the MAT, MAP and different extractable metals contents. The dashed and solid lines represent insignificant and significant fitted models, respectively. The shaded area represents the 95% confidence interval.  $k$  is the slope of the linear fitting analysis.

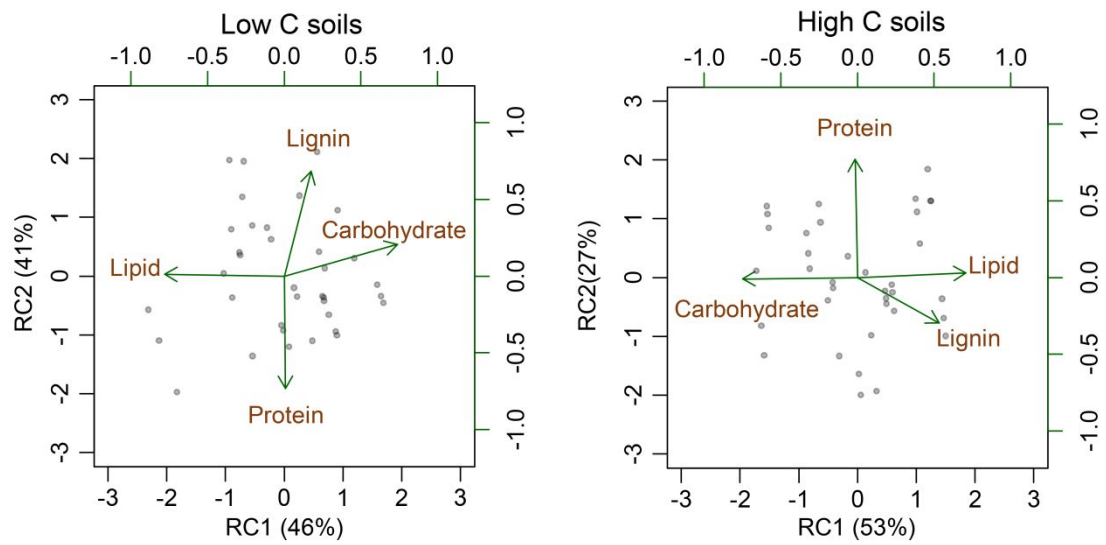


**Fig. S11.** RPCA of SOC molecules in low- and high-OC soils. RC1 and RC2 represent rotated components 1-2; panels indicate pairwise comparisons of RC1 and RC2. Gray dots represent soil samples, and labeled arrows indicate correlations between SOC molecules and RCs.

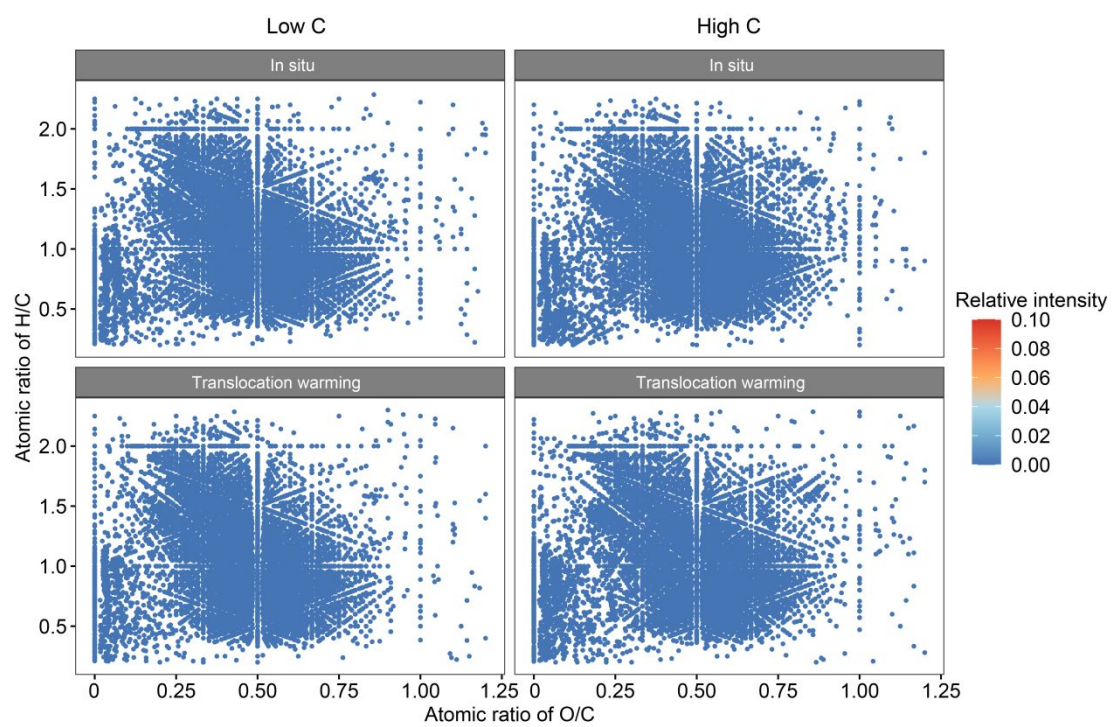


**Fig. S12.** van Krevelen Diagram (VKD) for all samples under *in situ* and translocation warming in both low- and high-C samples.

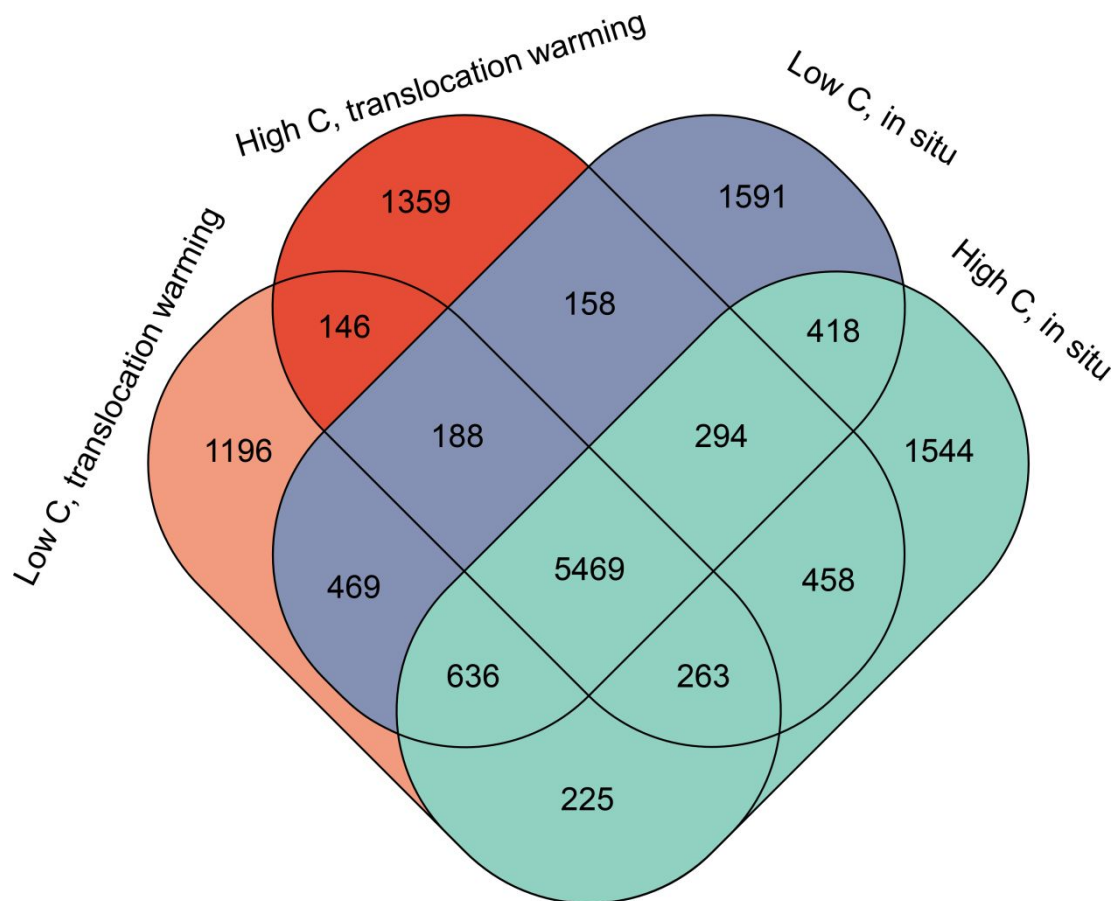


**Fig. S13.** Venn diagram of molecular formulae in dissolved organic matter (DOM) for all samples.



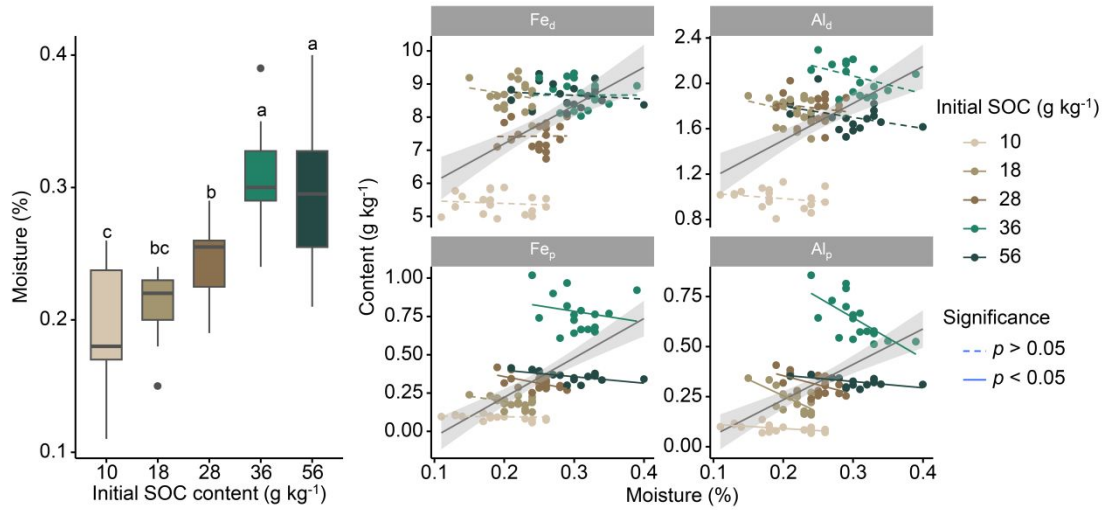


**Fig. S14.** Relationships between dithionite-citrate extractable Fe/Al, pyrophosphate extractable Fe/Al and soil moisture content. Different lowercase letters indicate significant differences, and the same lowercase letters indicate nonsignificant differences.

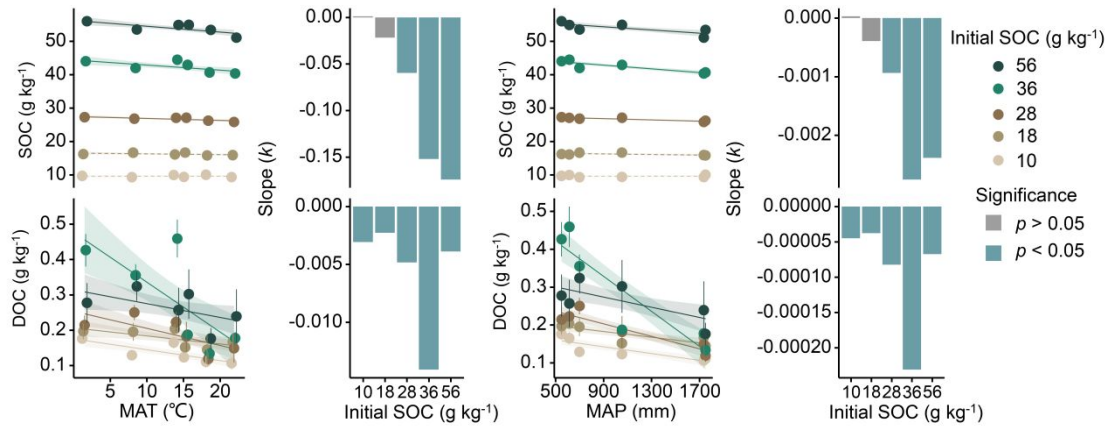


**Fig. S15.** Fitting relationships between soil organic carbon, dissolved organic carbon and MAT, and MAP.

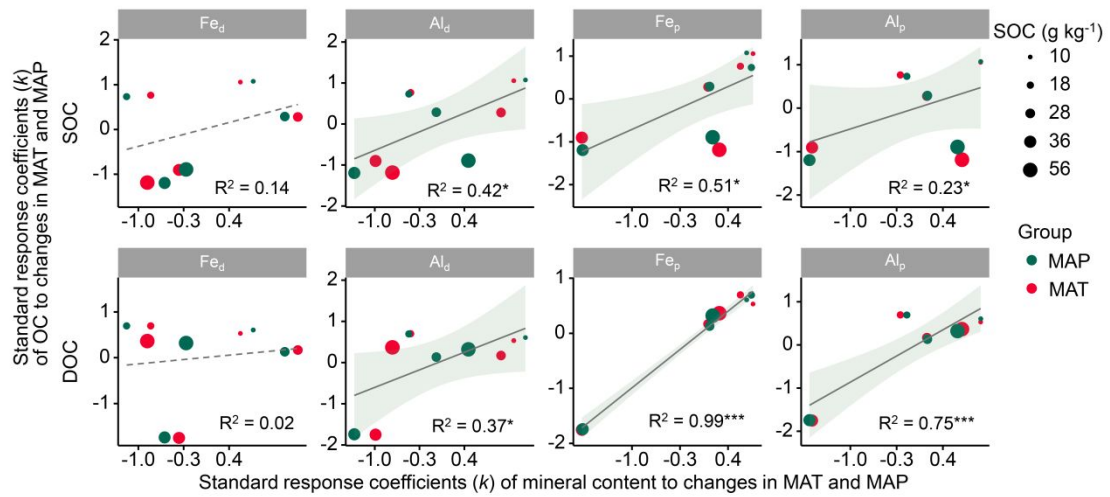


**Fig. S16.** Relationships between the response of organic carbon to translocations warming and the response of extractable Fe/Al to translocations warming. Response coefficients are from Fig. S9 and Fig. S14, respectively.